Earth and Planetary Science Letters xxx (2010) xxx–xxx

Contents lists available at ScienceDirect

Earth and Planetary Science Letters

journal homepage: www.elsevier.com/locate/epsl

Association between catastrophic paleovegetation changes during Devonian–Carboniferous boundary and the formation of giant massive sulfide deposits

Cesar Menor-Salván [a], Fernando Tornos [b,*], David Fernández-Remolar [a], Ricardo Amils [a,c]

[a] Centro de Astrobiología, CSIC-INTA, 28850 Torrejón de Ardoz, Madrid, Spain
[b] Instituto Geológico y Minero de España, Ríos Rosas 23, 28003 Madrid, Spain
[c] Centro de Biología Molecular "Severo Ochoa" (CSIC-UAM), Cantoblanco, 28049 Madrid, Spain

ARTICLE INFO

Article history:
Received 4 June 2010
Received in revised form 13 September 2010
Accepted 19 September 2010
Available online xxxx

Editor: M.L. Delaney

Keywords:
Iberian Pyrite Belt
volcanogenic massive sulfides
higher plant biomarkers
Devonian–Carboniferous boundary

ABSTRACT

The Iberian Pyrite Belt (SW Iberia) is one of the largest sulfur anomalies in the Earth's crust. In the southern Iberian Pyrite Belt, more than 820 Mt of exhalative massive sulfides were deposited in less than one million years at the Devonian–Carboniferous boundary. The shale of the ore-bearing horizon contains biomarkers indicating major biogenic activity in a methanogenic setting, including a five-fold increase in typical vascular plant biomarkers and a significant anomaly in those probably indicating the presence of thermophilic Archaea. This contrasts with signatures in the average sedimentary rocks of the basin that indicate the sediments settled in oxic to sub-oxic environments, and that they have only minor biomarkers derived from continental paleoflora. These data show that the formation of the mineralization was not only related to major hydrothermal activity synchronous with volcanism but may also have been controlled by the input of large amounts of organic matter, mostly derived from the degradation of woodland detritus sourced in the nearby continent. This massive influx of organic matter could have accelerated extremophilic microbial activity that used short-chain hydrocarbons as electron donors for seawater sulfate reduction, resulting in concomitant massive sulfide precipitation. We propose that the giant massive sulfide deposits resulted from overlapping of geological and biological processes that occurred at the Devonian to Carboniferous transition, including: (1) continent collision during the onset of the Variscan orogeny leading to major paleogeographic changes and volcanism; (2) dramatic stress of continental ecosystems due to the combination of climatic change, volcanism, variations in the sea level and erosion on a regional scale; (3) major biomass destruction and increase of organic supply to marine environments; and, (4) generation of anoxic conditions and the thriving of sulfate reducing microorganisms. Under these conditions, massive sulfide deposits formed where venting sulfur-poor but metal-rich hydrothermal brines flowed into a hydrogen sulfide-rich anoxic water column. The data presented strongly suggest that there was a temporal and causal relationship between the Devonian–Carboniferous geotectonic, climatic and biological crises and the formation of the giant volcano-sedimentary massive sulfide deposits of the southern Iberian Pyrite Belt.

1. Introduction

The Iberian Pyrite Belt (IPB) (Fig. 1) hosts one of the largest concentrations of volcano-sedimentary massive sulfide deposits on Earth, comprising 45% of the giant (>100 million tons of contained ore) deposits world-wide (Leistel et al., 1998; Tornos, 2006). Furthermore, it represents one of the largest crustal sulfur anomalies, mostly in the form of pyrite in the stratabound massive sulfide deposits (ca. 1730 Mt), the underlying (sub-) economic stockwork or feeder zone (ca. 300 Mt) and about 3000 Mt of hydrothermally altered volcanic and siliciclastic rocks with disseminated pyrite (Fig. 1). The ore deposits formed in a manner similar to that of present day submarine hydrothermal systems (Herzig and Hannington, 1995; Ohmoto, 1996). However, a major difference between present day systems and ancient ones is that most recent ones occur on oxic oceanic bottoms where the massive sulfides are rapidly oxidized and destroyed if they are not covered by sediments or volcanic rocks (Herzig and Hannington, 1995). Most ancient deposits occur in anoxic settings, where the massive sulfides not only accumulated but also were preserved. In fact, there was a close association between anoxic events and formation of sedimentary Zn–Pb sulfide deposits on the seafloor (Goodfellow, 1987; Goodfellow and Jonasson, 1984).

The aim of this work is to study the relationships between massive sulfide formation and the geochemistry of the hosting shale, by studying the biomarkers present in the ore-bearing and barren shale.

---

* Corresponding author.
E-mail address: f.tornos@igme.es (F. Tornos).

0012-821X/$ – see front matter © 2010 Elsevier B.V. All rights reserved.
doi:10.1016/j.epsl.2010.09.020

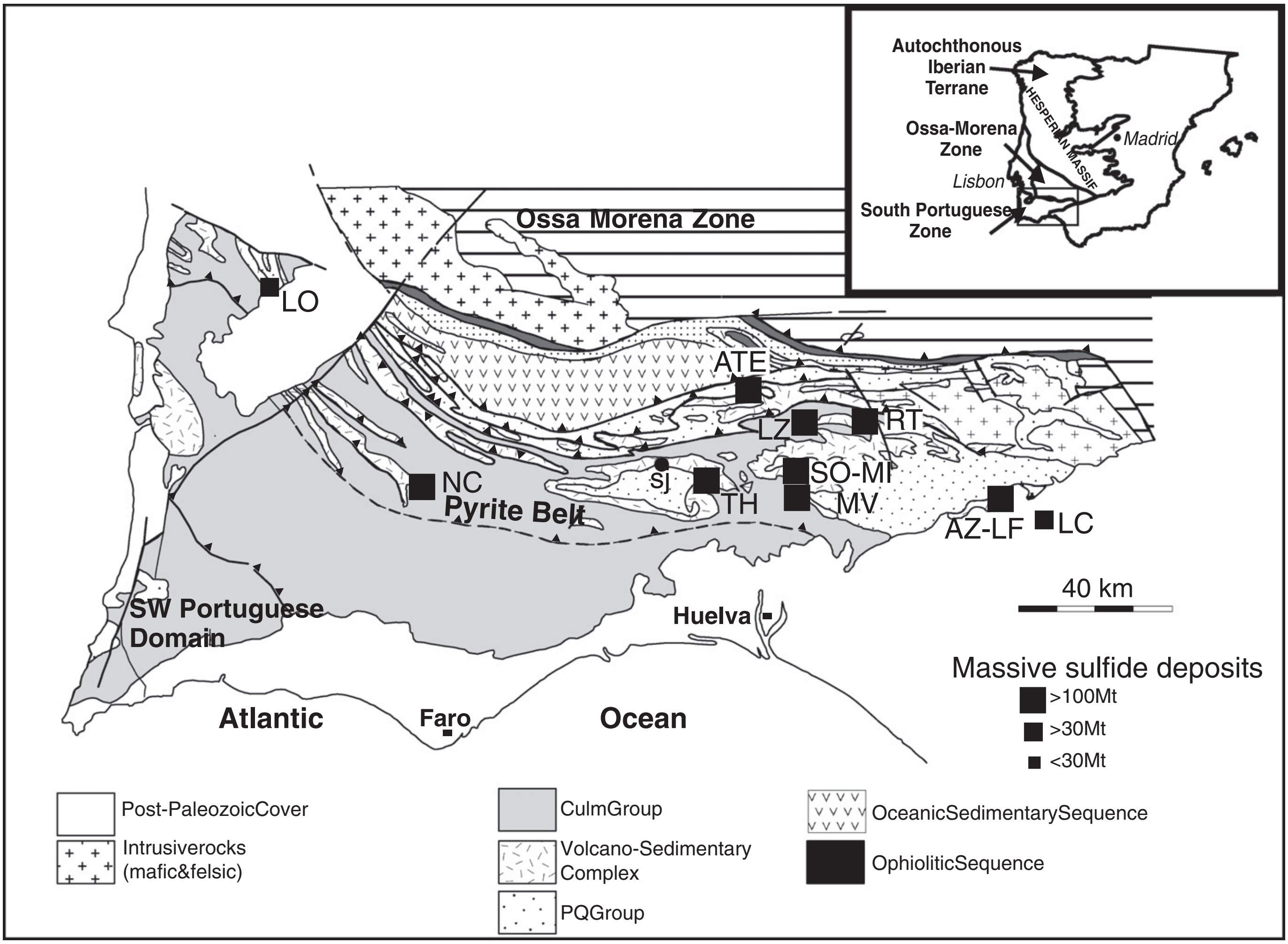

Fig. 1. Geological map showing the location of the major deposits described in the text and the location of the San Jorge section (sj). AZ-LF: Aznalcóllar-Los Frailes; LC: Las Cruces; LO: Lousal; LZ: La Zarza; NC: Neves Corvo; MV: Masa Valverde; RT: Rio Tinto; SO-MI: Sotiel-Migollas; TH: Tharsis. Modified from Tornos (2006).

The results presented here, in combination with geologic, isotopic, and SEM data, show the critical control exerted by biogenic activity in the formation of the volcanogenic massive sulfide deposits in the Iberian Pyrite Belt. These deposits formed during unusual paleogeographic conditions, coeval with a paleoclimatic crisis and active hydrothermal activity, producing an explosion of microbial life and formation of giant ore deposits.

2. Geologic setting

The massive sulfide deposits of the IPB formed synchronously with calc-alkaline volcanism during the early stages of the Variscan orogeny, when Avalonia started to amalgamate with Gondwana during late Devonian to early Carboniferous times (Silva et al., 1990). Continent–continent oblique collision led to the formation of pull-apart basins on both terrains. In the exotic Avalonia terrane the onset of deformation produced tectonic disturbance of a stable continental shallow platform where mature siliciclastic sediments, shale and quartz-arenite of the PQ Group (upper Givetian to Famennian) were deposited. Formation of half-graben basins led to heterogeneous and high energy sedimentation, represented by the local deposition of subaerial, fan delta, carbonate and gravity flow deposits during the uppermost Famennian (Moreno et al., 1996). These rocks are in part coeval with the Volcano-Sedimentary Complex, of late Devonian-middle Visean age, that comprise large andesite–rhyolite dome complexes and basaltic lava flows and sills interbedded with abundant shale and epiclastic and chemical sedimentary rocks (Leistel et al., 1998; Tornos, 2006).

The style of mineralization of the massive sulfide orebodies shows a major paleogeographic control. Massive sulfide deposits located in the northern part of the belt formed by sub-seafloor replacement of pumice- and glass-rich volcanic rocks, are unrelated to shale and are of early Visean age (Fig. 2); they are not further discussed in this paper. Those in the southern part are very different, since are hosted by shale, being exhalative in origin and formed in anoxic third order basins. Some of these deposits show abundant sedimentary structures indicating dominant precipitation on the seafloor as well as common mound-like structures made up of laminated and breccia-like pyrite–siderite rocks (Fig. 2) (Almodovar et al., 1998; Relvas et al., 2001; Tornos et al., 1998; 2008). The giant deposits of Neves Corvo, Tharsis, Masa Valverde, Aznalcóllar-Los Frailes, Las Cruces and Sotiel-Migollas, comprising in total about 820 Mt of massive sulfides, formed

Fig. 2. Relationships between geology, age, geotectonic evolution, paleogeography, and massive sulfide deposits in the Iberian Pyrite Belt. Chronostratigraphy based on the palynological data of Gonzalez (2005) and U–Pb dating of Dunning et al. (2002) ((1) in the figure) and Barrie et al. (2002) (2). The synorogenic facies of the D–C transition include the subaerial, fan delta, carbonate and gravity flow deposits of the uppermost PQ Group (Moreno et al., 1996). The column includes the location of the shale-hosted and volcanic-hosted massive sulfide deposits, of late Famennian and late Tournaisian age, respectively.

Please cite this article as: Menor-Salván, C., et al., Association between catastrophic paleovegetation changes during Devonian–Carboniferous boundary and the formation of giant massive sulfide deposits, Earth Planet. Sci. Lett. (2010), doi:10.1016/j.epsl.2010.09.020

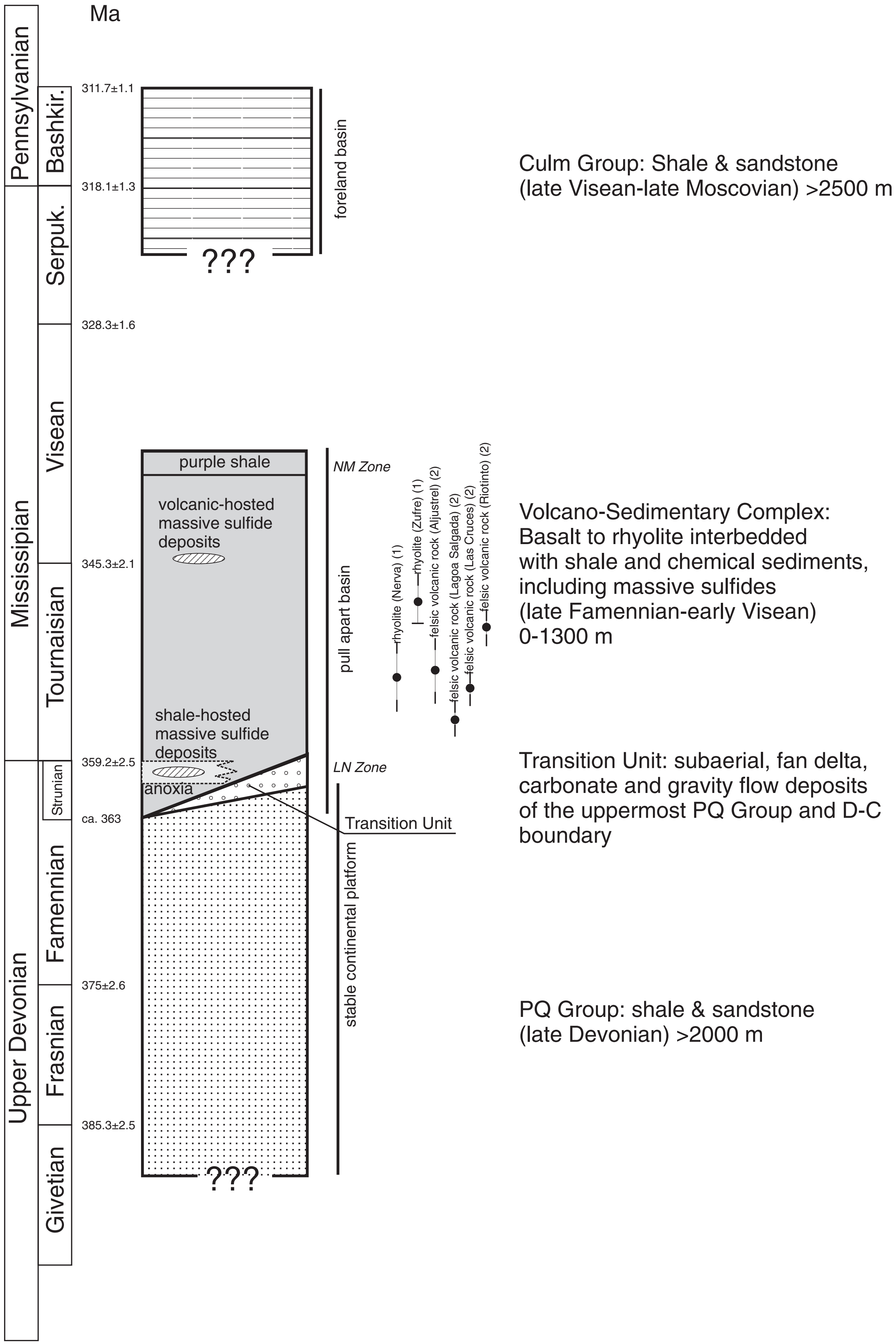

Please cite this article as: Menor-Salván, C., et al., Association between catastrophic paleovegetation changes during Devonian–Carboniferous boundary and the formation of giant massive sulfide deposits, Earth Planet. Sci. Lett. (2010), doi:10.1016/j.epsl.2010.09.020

synchronously with, or just after the first recorded volcanic activity in the area. There are few macrofossils but systematic palinological dating of the shale hosting these orebodies (Gonzalez et al., 2006; Oliveira et al., 2003; Pereira et al., 1996 and references therein) shows that the shale-hosted massive sulfides formed during the LN biozone, the uppermost biozone of the Strunian (363–359 Ma, latermost Devonian) (Streel et al., 2006). This indicates that the shale-hosted massive sulfide deposits formed in a brief time span of less than 1 Ma and just before (if not within) the Devonian–Carboniferous (D–C) boundary, coinciding with major paleogeographic changes and the onset of volcanic activity (see Moreno et al., 1996; Silva et al., 1990) (Fig. 2).

Fluid inclusion data indicate that the ore forming fluids had salinities between 3 and 12 wt.% NaCl eq. Calculated $\delta^{18}O$-δD values of ore forming fluids, in the range of 0 to 8‰ and −45 to 5‰ respectively, and Pb ($\mu = 9.8$–10), Sr ($^{87}Sr/^{86}Sr_{initial}$, 0.7021–0.7221), and Os ($^{187}Os/^{188}Os_{initial} \approx 0.69$) initial values of the mineralization and related hydrothermal alteration are consistent with equilibration of fluids at low fluid/rock ratios with long lived and evolved continental crust, represented by the sedimentary rocks of the PQ Group and/or the underlying basement (Tornos, 2006). The ore forming fluids were not modified, convected and heated seawater that interacted with sediments and volcanic rocks leaching sulfur and metals, as stated for most volcanic-hosted massive sulfide deposits (e.g., Herzig and Hannington, 1995; Lydon, 1988; Ohmoto, 1996), but are interpreted to be derived from the rapid dewatering and accelerated diagenesis/low grade metamorphism of the underlying siliciclastic sequence, probably directly related to crustal thinning, magma intrusion and increase of the geothermal gradient (Tornos, 2006).

Numerical modeling suggests that hydrothermal fluids that equilibrated with shale containing intermediate redox assemblages are metal-rich but sulfur-poor; these fluids travelled through the crust until they were mixed with a H_2S-rich fluid, leading to the precipitation of sulfides and the formation of the massive sulfide deposits (Tornos and Heinrich, 2008). Saline fluids discharged from hydrothermal vents accumulated as brine in bathymetric depressions on the seafloor (Sato, 1972) at temperatures between 60 and 120 °C (Tornos et al., 1998). This temperature range is close to that of steady state equilibrium in brine pools (Solomon et al., 2004) and to the optimal growth conditions for thermophilic microorganisms (Stetter, 1999).

Data supporting this model include the systematically low and variable $\delta^{34}S$ (between −34 and +21‰) values in the shale-hosted massive sulfide deposits if compared with those in the stockwork zones (−2.5 to +10‰) (Tornos, 2006; Velasco et al., 1998) and the presence in the stockwork of mineral assemblages typical of sulfur-poor environments, such as tellurides, pyrrhotite, Co–As-bearing minerals and arsenopyrite that are not found in the overlying stratabound massive sulfide deposits (Marcoux et al., 1980; Tornos et al., 1998). The sulfur isotope values of the exhalative ores are interpreted as reflecting mixing of sulfur from two contrasting sources, one of deep origin and another produced by biogenic seawater sulfate reduction under fluctuating open and closed conditions within an anoxic basin. The deep upflowing hydrothermal fluids leached metals and limited amounts of sulfur from the underlying sediments; mass balance calculations suggest that up to 50% of the sulfur was added at the site of massive sulfide formation. A biogenic source of this sulfur is consistent with an evidence of widespread biologic activity in the ore forming environment, including the presence of probable worm burrows some cm above the footwall of the massive sulfides, the formation of siderite–pyrite laminated mounds interpreted as fossil microbial mats (Tornos et al., 2008) and the presence of microfossils that may represent pyritized microbial shells. These late structures (Fig. 3) are likely of organic origin and too small to be spores.

Although this model may explain the formation of the massive sulfide deposits, it does not satisfactorily explain the mass and charge balance, as biogenic reduction of seawater sulfate requires a reducing agent. The most likely one is methane, but Tornos and Heinrich (2008) concluded that the deep hydrothermal fluids must be weakly reduced to oxidize in order to transport large amounts of metals, thus ruling out the presence of high contents of CH_4. Therefore, one of the key questions related to massive sulfide formation in the IPB is the source and nature of the reductant.

The drillhole PG-1 (37°36′34″N; 7°11′58″W) is located about 8 km west of the giant Tharsis deposit with about 115 Mt of massive sulfides, mostly as pyrite. This 290 m long drillhole intersected a 10 m thick pyrite-rich massive sulfide lens within a 120 m thick sequence of shale belonging to the lowermost Volcano-Sedimentary Complex that is interpreted as being a lateral equivalent of the Tharsis orebody (Tornos et al., 2008). In both cases, the ore-bearing interval coincides with a zone of major chemical changes at the basin scale (Fig. 5). The shale shows a sharp increase in the Na_2O/K_2O ratio, probably related to the input of detritus from the growth of the first volcanic edifices within the basin, accompanied by a dramatic drop in the Mn and Fe contents and an increase in the V/Cr ratios that are indicative of anoxic conditions. Highly reducing, even methanogenic, conditions are inferred from the high V (>300 ppm) contents, high V/Cr (>4.3), V/Ni (>4.7) ratios and low Mn (<260 ppm) contents and the absence of barite in the ore assemblage. Furthermore, the shale shows a synchronous decrease in $\delta^{34}S$ values from the highly variable values of −21 to 3‰ of the regional shale to constant and low values of −29 to −27‰ in the ore-bearing horizon (Tornos et al., 2008). These data are consistent with ore formation taking place during a short-lived highly anoxic event that was coeval with major microbial activity and the onset of the volcanism. Shale ca. 1–2 m above the massive sulfides has V, Ni, Mn, Fe and Cr contents typical of shale deposited in sub-oxic to oxic conditions indicating that anoxic conditions were thus strictly coeval with the precipitation of the massive sulfides. The results presented here are interpreted as having a regional significance, since the geochemistry of shale is shown to be homogeneous at the basin scale (e.g., Nägler, 1990), something that is also consistent with the existence of a well defined ore forming horizon all along the southern Iberian Pyrite Belt.

3. Methods

3.1. Samples

Core from drillhole PG-1 stored at the facilities of the IGME at Peñarroya (Spain) was systematically sampled by sawing half cores of the shale-rich units. About ½ kg of whole rock from 56 samples was later powdered and analyzed for major and trace elements, stable sulfur isotopes and total organic carbon (TOC).

3.2. Extraction and fractionation of the organic matter

About 80 g of pulverized sample was placed in a reactor with a mixture of dichloromethane and methanol (7:1 v:v) for 8 h using a programmable hot extraction system (Büchi B-811 model). Samples were concentrated to 1 ml and desulfurized in an elemental copper powder column previously activated with 2 M HCl. After removing elemental sulfur, the solvent was removed to yield the extract for analysis. The crude extract was placed at the top of a silica column (2 ml, filled with chromatography grade silica, 0.063–0.2 mm particle diameter). Saturated and aromatic fractions were eluted with 10 ml of n-pentane:dichloromethane (4:1). A second polar fraction was eluted with 10 ml of pure dichloromethane. The separated fractions were dried under N_2 and re-dissolved in 150 µl of dichloromethane.

Please cite this article as: Menor-Salván, C., et al., Association between catastrophic paleovegetation changes during Devonian–Carboniferous boundary and the formation of giant massive sulfide deposits, Earth Planet. Sci. Lett. (2010), doi:10.1016/j.epsl.2010.09.020

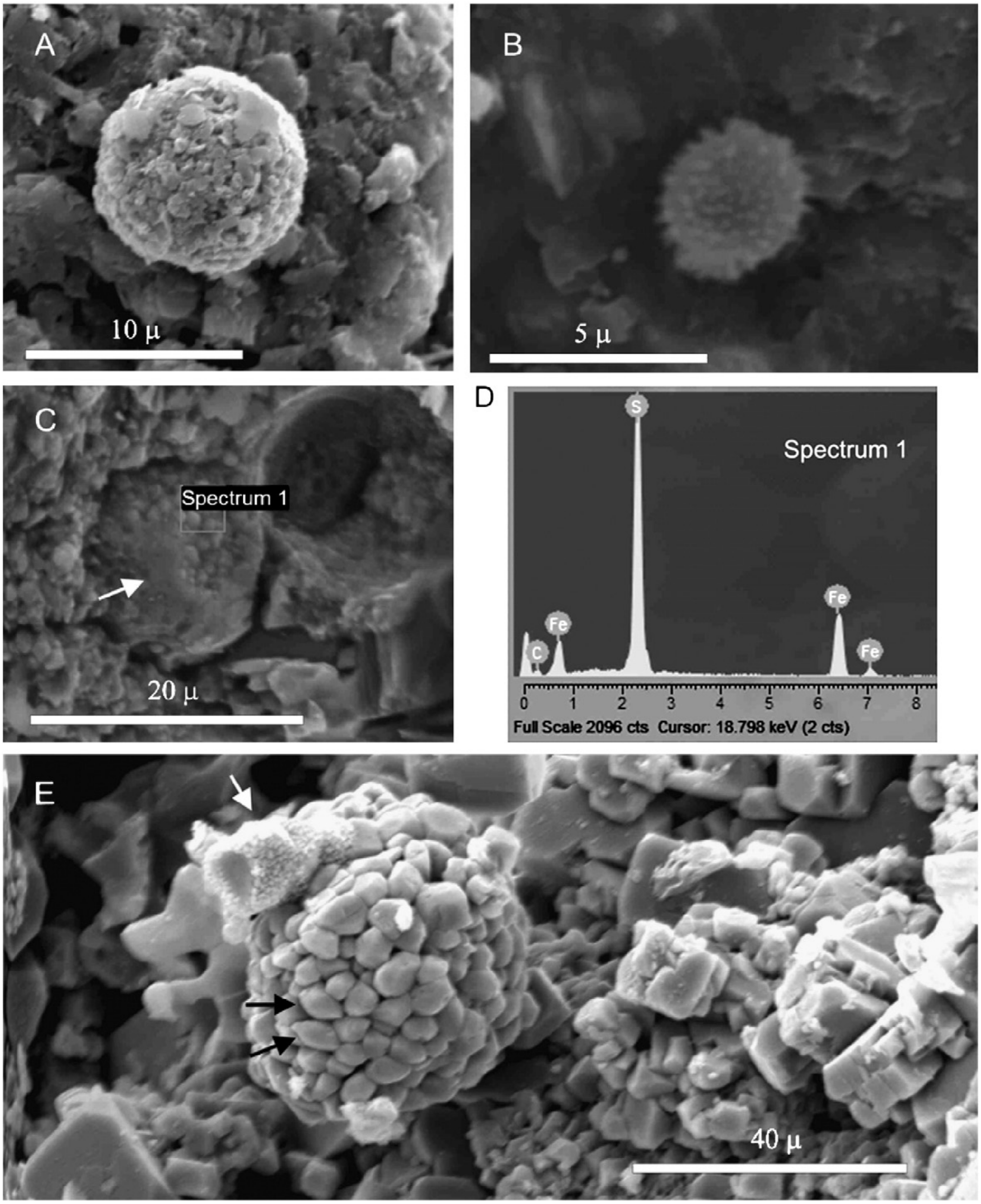

Fig. 3. SEM-EDS analysis of different samples obtained in the Tharsis Filón Norte massive sulfide orebody show evidences of microbial activity supporting sedimentary origin. A) Framboidal structure covered partially by a Si-rich coating with some traces of carbonaceous matter. B) Organic microfossil of unknown origin with spinose projections resembling bacterial spores or small-sized acritarchs. C) Pyritic framboid covered by a carbonaceous lamina and which mineral units are internally embedded inside an organic matrix. D) EDS spectrum obtained from the framboid shown in (C), where is compositionally dominated by sulfur and iron (pyrite) and organic carbon (no oxygen detected) supporting the occurrence of organics associated to some framboidal structures. E) Pyrite framboid associated to a spinose organic-walled microfossil (with arrow), where some micron-sized mineral units show apicular termination (see black arrows) as observed in some microbial structures casted by mucilaginous films (Gong et al., 2008).SEM-EDS analysis of ore from the Tharsis Filón Norte massive sulfides showing evidences of microbial activity. A) Framboidal structure coated swith silica (black arrows) with traces of carbonaceous matter. B) Microfossil of unknown origin with spinose projections resembling fungi as found by Jackson et al. (2009). C) Pyrite framboid covered by a carbon-rich film with the individual crystals embedded in organic matter. D) EDS spectrum of the framboid shown in (C), composed of sulfur, iron and organic carbon (no oxygen detected) supporting the occurrence of organic matter associated with some framboidal structures. E) Framboid of pyrite associated with a spinose organic-walled microfossil (arrow), where some micron-sized grains show apicular terminations (black arrows) similar to those of some microbial structures cast by mucilaginous films (Gong et al., 2008).

3.3. Gas chromatography-mass spectrometry (GC-MS)

The analyses were performed on an Agilent 6850 GC coupled to an Agilent 5975 C quadrupole mass spectrometer. Separation was achieved on an HP-5MS column coated with (5%-phenyl)-methylpolysiloxane (30 m × 0.25 mm, 0.25 µm film). The operating conditions were as follows: 8 psi carrier pressure, initial temperature held at 40 °C (1.5 min), increased from 40 to 150 °C at a rate of 15 °C/min, held 2 min, increased from 150 to 255 °C at a rate of 5 °C/min, held for 20 min and a final increase to 300 °C at a rate of 5 °C/min. The sample

Please cite this article as: Menor-Salván, C., et al., Association between catastrophic paleovegetation changes during Devonian–Carboniferous boundary and the formation of giant massive sulfide deposits, Earth Planet. Sci. Lett. (2010), doi:10.1016/j.epsl.2010.09.020

was injected in splitless mode with the injector temperature at 290 °C. The mass spectrometer was operated in electron impact mode (EI) at 70 eV ionization energy, scanned from 40 to 700 Da and operated in SIM mode at m/z 85, 183, 219 and 197. Temperature of the source was 230 °C and quadrupole temperature was 150 °C. Data were acquired and processed with Chemstation software. Individual compounds were identified by comparing their mass spectra with those of standards and with published data.

4. Organic geochemistry of the ore-bearing sequence

Biomarker analysis of rock samples from the PG-1 drillcore was performed to elucidate the biological sources of the organic matter in the basin. Shale from the ore-bearing horizon contains 0.045 ± 0.005% of mean extractable organic matter which is composed mainly of saturated, linear and branched hydrocarbons, unspecific aromatic compounds and bacterial and plant biomarkers (Fig. 4). A clear quantitative increase in the biomarkers produced by plant degradation was observed in the ore-related samples when compared with barren rocks below and above the orebody (Fig. 5).

4.1. Higher Plant Index

The three aromatic biomarkers selected for the study of variation in higher plant input were cadalene (4-isopropyl-1,6-dimethylnaphthalene), retene (1-methyl-7-isopropylphenanthrene) and ip-iHMN (6-isopropyl-1-isohexyl-2-methylnaphthalene). These three compounds have natural precursors abundant in extant plants (Peters et al., 2005; van Aarssen et al., 1996, 2000). The Higher Plant Index was calculated using the equation:

$$HPI = ([\text{retene}] + [\text{cadalene}] + [\text{ip} - \text{iHMN}])\,([\text{TeMN}])^{-1}$$

Where TeMN is the bacterially derived 1,3,6,7-tetramethylnaphthalene, used to correct the higher plant input with bacterial inputs at the same maturation grade. The quantification was performed using the mass fragments at m/z 219 for retene, m/z 183 for cadalene, m/z 197 for ip-iHMN and m/z 169 for TeMN respectively.

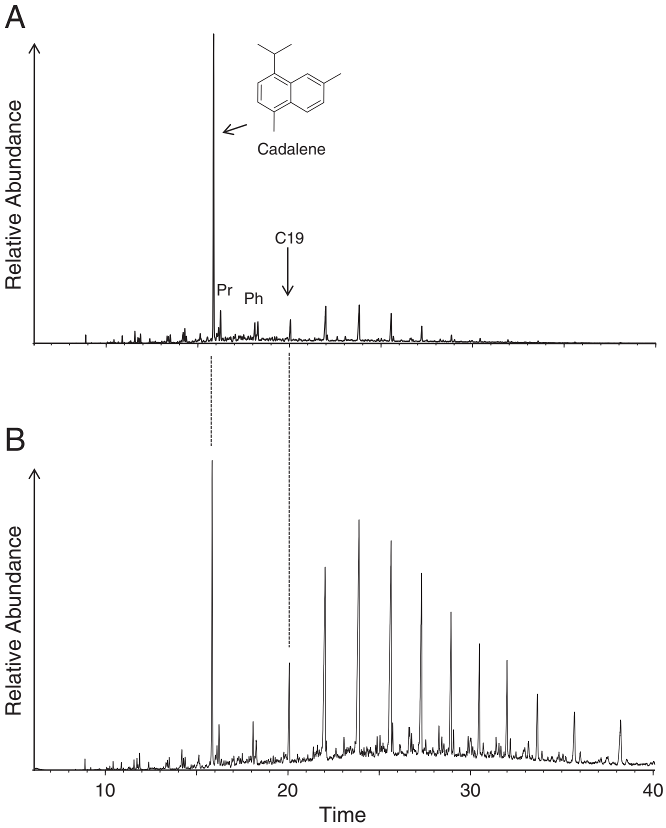

Fig. 4. GC-MS trace in SIM mode at m/z 183 and 85 of the aliphatic/aromatic fraction. A: sample from level 84 m, showing a high relative abundance of cadalene with respect to n-alkanes. B: sample at level 26.15 m, above the mineralization, at the stabilization zone of the higher plant input. The abundance of cadalene relative to n-alkanes is lower above and below the orebody. C19: n-nonadecane; Pr: pristane; and Ph: phytane.

A five-fold increase in the Higher Plant Index (HPI) was observed in the ore-bearing horizon, in the same trend with the individual higher plant biomarkers (Fig. 5). The HPI increase suggests a higher input of vascular plants to the sediments. This major change is accompanied by an increase in the 2-methylretene/9-methylphenanthrene ratio; 2-methylretene has been interpreted as a gymnosperm marker through diagenesis of abietane and phyllocladane class diterpenes. To assess the possible effect of differential maturation in the orebody, the values of the biomarker were corrected using the ratio with the unspecific maturation product 9-methylphenanthrene (Bastow et al., 2001).

4.2. Branched alkanes with quaternary carbon

Shale samples from the ore-bearing horizon are significantly enriched in 5,5-diethyl-alcane hydrocarbons including 5.5-diethyl pentadecane and 5,5-diethyl-tridecane (Fig. 6). The biosynthetic origin of quaternary diethyl alkanes has been demonstrated, but the source organisms are unclear due to the scarcity of these structures in modern environments. The presence of branched quaternary carbons in modern deep sea hydrothermal waters suggests that they may be biomarkers for non-photosynthetic reducing thermophilic prokaryotes or Archea (Kenig, 2003, 2005). Also, these molecules may be indicators of the response of source organisms to environmental changes, as euxinic to oxygenated water columns lack quaternary carbon branched alkanes, indicating low oxygen concentrations (Kenig, 2003).

4.3. Paleovegetation proxies

The analysis of organic extracts from samples obtained at the bottom of and below the mineralized horizon gave relatively low HPP (Higher Plant Parameter) values. This parameter is expressed as the abundance of retene relative to the sum of retene and cadalene, measured at m/z 219 (retene) and m/z 183 (cadalene). HPP is used as a tracer of the evolution or changes of paleovegetation, as the increase of gymnosperm input leads to an increase of HPP (Fleck, 2002; van Aarssen et al., 2000). This inference is based in the origin of cadalene, a diagenetic product of cadinene, the common product of sesquiterpenoid biosynthetic pathway and considered a generic vascular plant biomarker. Retene is the final diagenetic product of the abietane-class diterpenes, characteristic products of gymnosperm secondary metabolism. Hence, the reduced level of HPP in the orebody reflects a decrease in gymnosperm contribution to the terrigenous input of organic matter. These reduced levels could be related to severe alteration of ecosystems at the beginning of the mineralization period, followed by a recuperation of the gymnosperm dominance reflected as an increase in HPP values.

The decrease of HPP in the initial stages of black shale deposition and orebody formation is consistent with the increase in cadalene in the ore-bearing horizon (Fig. 5). The ratio cadalene/n-nonadecane is used to correct the variation of cadalene in relation to variations in total extractable organic matter and errors in sample manipulations, as n-nonadecane levels relative to the total peaks found do not show

Please cite this article as: Menor-Salván, C., et al., Association between catastrophic paleovegetation changes during Devonian–Carboniferous boundary and the formation of giant massive sulfide deposits, Earth Planet. Sci. Lett. (2010), doi:10.1016/j.epsl.2010.09.020

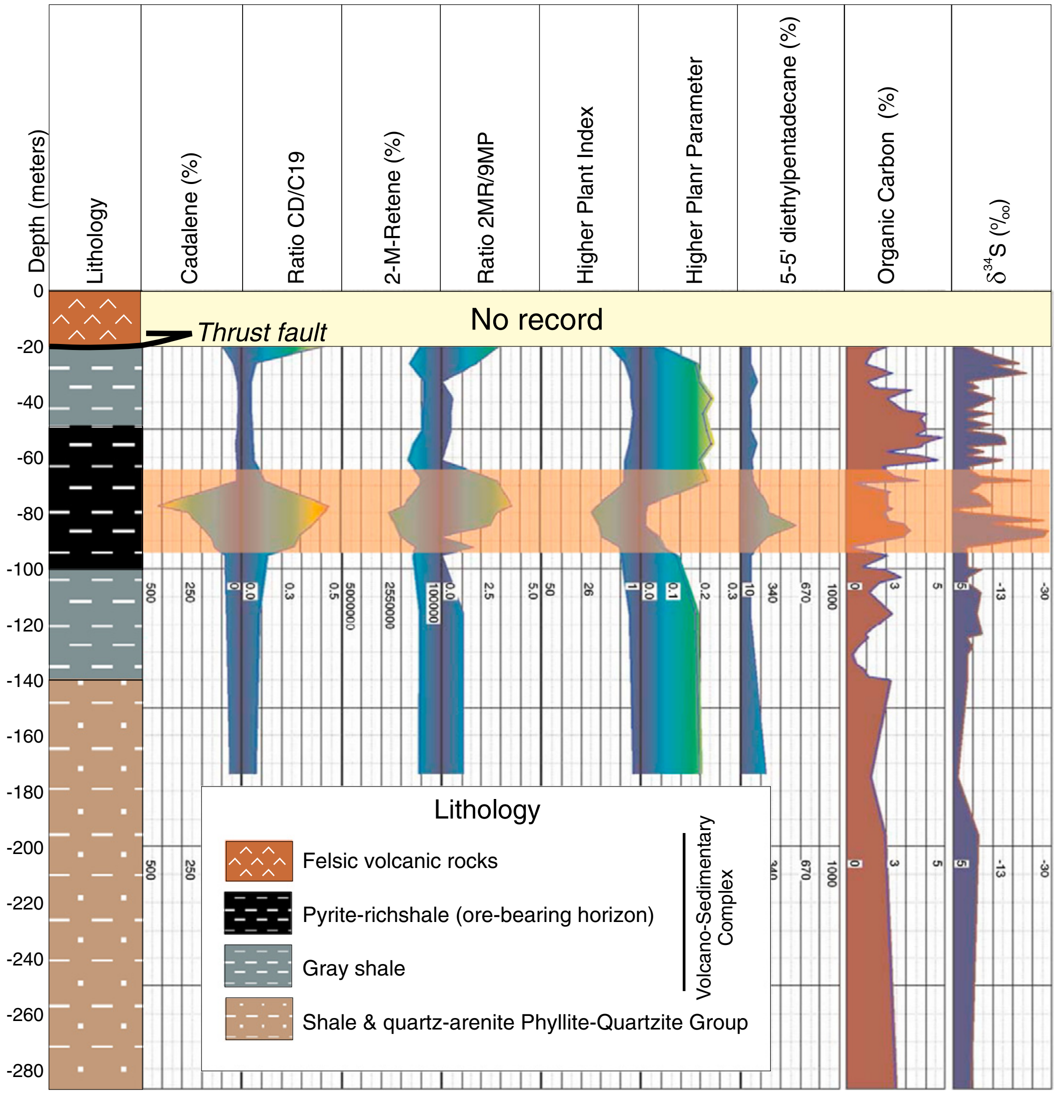

Fig. 5. Composite stratigraphic column of the San Jorge section showing variations of some key geochemical parameters with depth. CD/C19: ratio cadalene/n-nonadecane; 2-M-Retene: 2-methylretene; and 2MR/9MF: ratio 2-methylretene/9-methylphenanthrene.

variation along the drillcore studied. This ratio could also be indicative of the higher plant (terrigenous)/algal (marine) ratio and show the same trend in vertical variation as the terrigenous/aquatic ratio (TAR), calculated using the distribution of odd n-alkanes (Peters et al., 2005). The increase of TAR in the orebody must be taken with caution, as the n-alkane ratios are sensitive to secondary, post-depositional processes and its usage is normally restricted to young sediments. Despite these qualifications, the variation of TAR with the same trend as the other indicators is consistent with the increase of terrigenous material input to the basin.

In the later stages of the mineralization period there is a second major and similar biogeochemical discontinuity. Samples above the pyritic shale-gray shale contact at ca. 55 m. in drillhole PG-1 (Fig. 5) are also characterized by an abrupt increase in HPP and dehydroabietic acid, which is a diagenetic product of abietic acid also indicative of gymnosperms (Otto and Simoneit, 2001). Given that the dehydroabietic acid and dehydroabietanes enrichments correlate with higher HPP values, and the lack of dehydroabietanes in the shale below ca. 55 m, it can be deduced that the continental ecosystem was dominated by new species of gymnosperm-like plants during the later stages of ore formation (Fleck, 2002).

4.4. Plant biomass input sourced from terrestrial ecosystem destruction

To determine the continental biomass that was consumed by microbial activity, we considered a simple biogeochemical reaction involving a six carbon molecule of glucose that is the molecular base for cellulose. This mechanism results from activation of the sulfate ion by adenosine triphosphate (ATP), which is catalysed by the enzymes ATP sulfurylase and APS reductase. In dissimilatory sulfate reduction mediated by microbes, the electrons are transferred by a hydrogenase to the low potential cytochrome c3 that releases electrons to a cytochrome complex, which is the final stage of reduction to sulfide. Glucose was selected as the potential electron donor given that some hyperthermophilic and sulfate-reducing archaea can reduce sulfate through incomplete oxidation of glucose to produce acetate and CO_2

Please cite this article as: Menor-Salván, C., et al., Association between catastrophic paleovegetation changes during Devonian–Carboniferous boundary and the formation of giant massive sulfide deposits, Earth Planet. Sci. Lett. (2010), doi:10.1016/j.epsl.2010.09.020

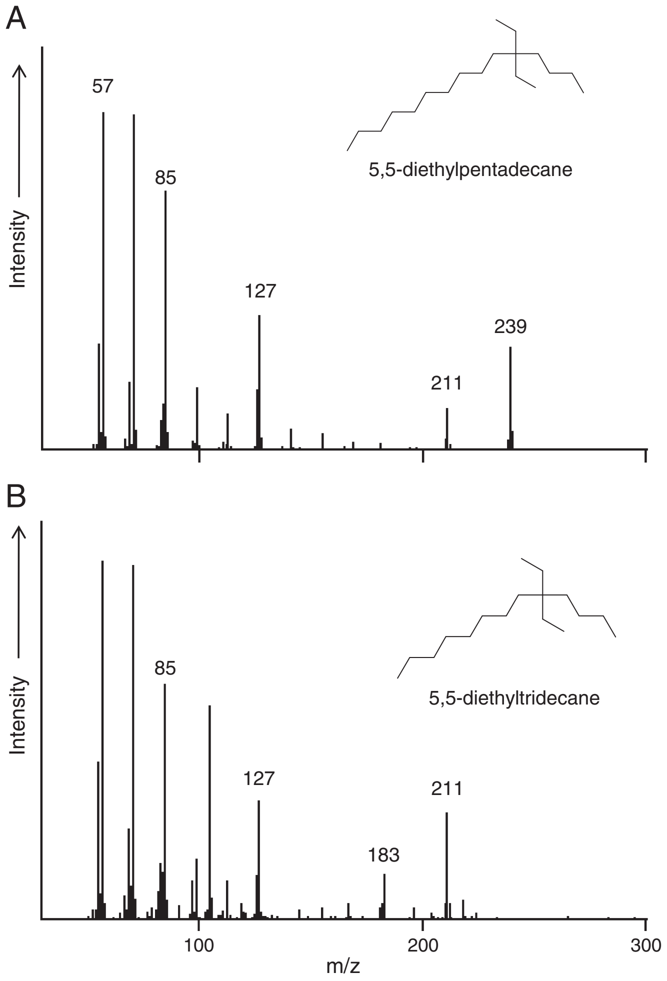

Fig. 6. Mass spectrum and structure of 5,5-diethylpentadecane (A), corresponding to the peak observed at 18.18 min in the fractionated extracts, and 5,5-diethyltritecane, observed at 14.3 min in the fractionated extracts (B). Identification based on data published in Kenig (2005). These compounds are the major branched alkanes with quaternary carbon (BAQCs) observed in samples.

(Labes and Schönheit, 2001). However, the acetate could be further oxidized by other sulfate reducing bacteria to CO_2 as has been observed in different microbial communities (Monetti and Scranton, 1992). Having these pathways in mind the reactions to produce pyrite mediated by microbes are the following:

$$C_6H_{12}O_6(\mathrm{glucose}) + SO_4^{=} \rightarrow 2{\bullet}CH_3COO^{-}(\mathrm{acetate}) + H_2S + 2{\bullet}CO_2 + 2{\bullet}H_2O \quad (1)$$

$$CH_3COO^{-}(\mathrm{acetate}) + SO_4^{=} + 3{\bullet}H^{+} \rightarrow H_2S + 2{\bullet}CO_2 + 2{\bullet}H_2O \quad (2)$$

$$H_2S + 0.5Fe^{2+} + 0.25O_2 \rightarrow H^{+} + 0.5{\bullet}FeS_2(\mathrm{pyrite}) + 0.5{\bullet}H_2O \quad (3)$$

which can be combined into the main reaction to produce pyrite synchronous with the release of CO_2

$$C_6H_{12}O_6 + 3{\bullet}SO_4^{=} + 1.5{\bullet}Fe^{2+} + 3{\bullet}H^{+} + 0.75{\bullet}O_2 \rightarrow 1.5{\bullet}FeS_2 + 6{\bullet}CO_2 + 7.5{\bullet}H_2O \quad (4)$$

The clearest evidence for this process is provided by the siderite–pyrite laminated ores and related breccias that are interpreted as fossil biogenic mounds (Tornos et al., 2008). The formation of siderite was favored by an increase in the pCO_2, generated as a by-product during the microbial reduction of seawater sulfate to H_2S and concomitant oxidation of organic matter to CO_2 due to the simplified reactions

$$CH_3COOH + SO_4^{=} + 2{\bullet}H^{+} \Leftrightarrow H_2S + CO_2 + 2{\bullet}H_2O \quad (5)$$

with the produced H_2S reacting with metals and precipitating the sulfides.

There is no major increase in the total organic carbon in the ore-bearing horizon when compared with the adjacent rocks (Fig. 5). This may indicate that amount of formed pyrite was limited by the availability of organic matter required as an electron donor in the reaction (4). Assuming that all the sulfide orebody is genetically associated with the destruction of organic matter, it is possible to calculate a maximum amount for the organic carbon that was involved in the reaction. Total original reserves of the Tharsis deposit were about 115 Mt of almost massive pyrite, of which roughly 105 Mt corresponds to sulfides and 10 Mt to siderite. This implies the presence of 56 Mt of sulfur (around 5.6×10^{13} g S) contained in the pyrite, which is the amount that has been used to estimate the total organic carbon consumed by sulfate reduction. Using Eq. (4), the total moles of carbon degraded by microbes is half of the total moles of sulfur, which results in 8.75×10^{11} C moles and around 1.05×10^{13}C grams. Assuming that carbon in siderite is derived from the CO2 generated in the Eq. (4), direct estimations provide around 10^{12} C grams. Adding both sources of carbon, siderite and pyrite, we estimate that destruction of the Late Devonian ecosystems provided up to 1.15×10^{13} C grams to the thermophilic communities in less than one million of years.

Some spectacular findings in early Carboniferous deposits (Falcon-Lang, 2004) provide information that allows us to make a rough estimation of the extent of the terrestrial ecosystems that were destroyed by the geotectonic processes required to produce the deposits in the Pyrite Belt. Falcon-Lang's paper gives data concerning the size, morphology and density of trees and forests in the earliest Carboniferous ecosystems. One important parameter is the mean tree diameter that is used to calculate the total stored carbon per tree by using different equations (Aparecida Vieira et al., 2009; Chave et al., 2005). The Mississippian woodlands described by Falcon-Lang (2004) had a trunk diameter averaging 6.26 cm and a tree density of around 1.8 x 10^6 trees per km^2. The application of the equation of Chave et al. (2005) allows us to calculate the number of trees on the basis of the total carbon consumed, as inferred from the size of the massive sulfide deposits. In this equation ($\mathrm{LnB} = -2.43 + \mathrm{lnD}$) a regression between biomass B (Kg) and tree diameter D (cm) implies up to 5.75×10^9 trees, which corresponds to an area of 3200 km^2 based on the average tree density calculated by Falcon-Lang (2004).

Fig. 7. Cartoon showing the development and destruction of the late Devonian terrestrial ecosystems during the onset of the Variscan orogeny in the area. a, Diagram showing Famennian (late Devonian) ecosystems dominated by progymnosperms, lycopsids, equiseta and ferns (see Algeo et al., 2001) with different water requirements from wet to drier conditions as in some modern ecosystems. The distribution of vegetal communities would have been arranged according to the regional geomorphology that controlled the topology and depth of the phreatic level in the substrate. At this stage we believe a regular phreatic level was likely, which is consistent with stable terrestrial communities, but there were also shallow inter-deltaic marine sedimentary areas producing carbonates (Moreno et al., 1996). b, Diagram showing dramatic changes in landscape affecting the terrestrial biota by the first stages of the Variscan orogeny, which induced compartmentation by formation of pull-apart basins and active volcanism. Combination of both processes induced several mechanisms such as (1) production of acid rain and dark effect, (2) disturbance of the phreatic level and regional climate by uplift and deepening, and, (3) rapid increase in erosion rates. Together, these actions worked to increase the supply of organic matter to the ocean. The gray tones in the massive sulfides include both the carbonate ore (light) interpreted as precipitated as biogenic mounds and the fine grained ore (dark), probably formed by direct fallout of sulfides from the chemocline.

Please cite this article as: Menor-Salván, C., et al., Association between catastrophic paleovegetation changes during Devonian–Carboniferous boundary and the formation of giant massive sulfide deposits, Earth Planet. Sci. Lett. (2010), doi:10.1016/j.epsl.2010.09.020

5. Interpretation

The data presented here indicate that the massive sulfide deposits of the Iberian Pyrite Belt formed synchronously with major changes in the biota and a major input of tree detritus from the nearby continent into the ocean. In detail, they formed in third order basins where hot, mildly reduced, metal-rich but H_2S-poor hydrothermal fluids accumulated and dissimilatory biogenic reduction of seawater sulfate

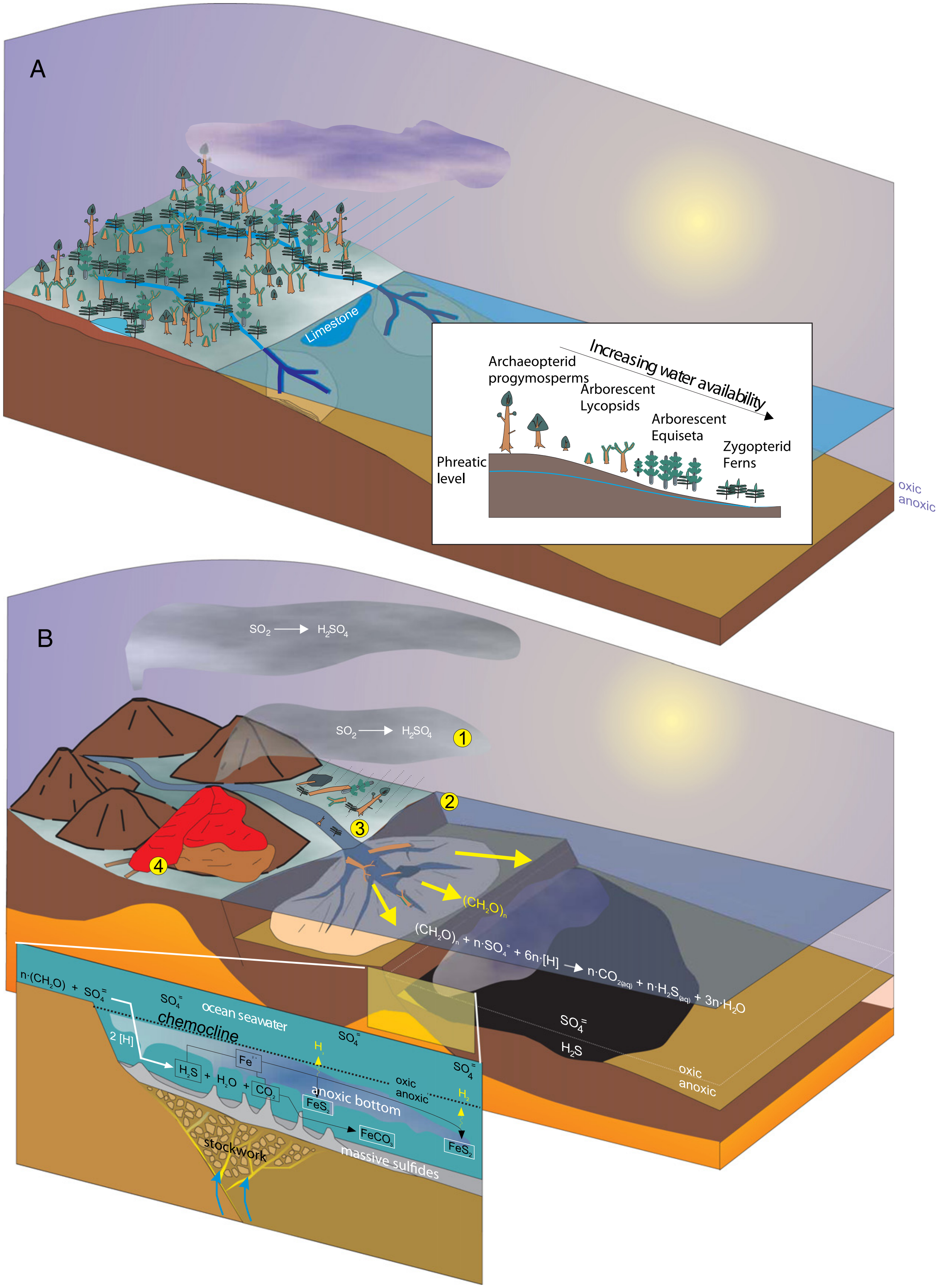

Please cite this article as: Menor-Salván, C., et al., Association between catastrophic paleovegetation changes during Devonian–Carboniferous boundary and the formation of giant massive sulfide deposits, Earth Planet. Sci. Lett. (2010), doi:10.1016/j.epsl.2010.09.020

became widespread (Goodfellow, 1987). Supplied organic matter acted as the critical electron donor needed for biogenic sulfate reduction and ore formation. Thermophilic archaea, such as *Archeoglobus* spp., reduced seawater sulfate to H_2S, thereby providing an almost unlimited supply of reduced sulfur to fix hydrothermal metals and form the massive sulfide deposits. Thus, input of large amounts of biomass into anoxic bottoms where submarine hydrothermal activity had already accumulated metal-bearing but sulfur-poor hot fluids favored microbial life explosion and highly effective formation of the giant massive sulfide orebodies.

The recorded change can only be related to a catastrophic event and with effects similar to those recorded at the KT boundary, where there is widespread evidence of major devastation and mass plant extinction (Johnson et al., 2000; Wilf and Johnson, 2004). The absence of retene-like biomarkers in the studied shale suggests that regionally extensive fires were not the main cause of forest destruction near the IPB. The ore-bearing horizon show only a slight increase in benz[a] anthracene, a possible biomarker for burning processes, but its presence alone is not conclusive.

The timing of hydrothermal activity and biomass destruction coincides with the Devonian–Carboniferous (D–C) boundary, one of the dozen major biota extinction events. The D–C boundary is related to the disappearance of about 21% of marine genera and the vanishing of sessile benthos and nektobenthic organisms, mainly most ammonoids, but also foraminifera, conodonts, brachiopods, corals and others (Caplan and Bustin, 1999; McLaren and Goodfellow, 1990; Sepkoski, 1996). This mass extinction was accompanied by an event of widespread anoxia (Hangenberg event) that has been tracked mainly at low paleolatitudes. Consistent with the Hangenberg event, our data shows an increase in branched hydrocarbons with quaternary carbon (BAQC). This increase could be the consequence of flourishing of organisms implicated in the sulfur cycle due to anoxia and increase of reduced carbon input, as BAQCs are considered indicators of environmental change to anoxic conditions (Bai et al., 2006; Kenig, 2003). Alternatives have been proposed for the D–C global extinction (Caplan and Bustin, 1999), including major volcanism, global cooling and warming, oceanic overturns, eutrophication, eustatic changes, or their combinations. Detailed isotopic studies show that climate warming and a rise in sea level due to melting of ice sheets followed an epoch of glaciation during the late Devonian (Kaiser et al., 2006). In such conditions, water circulation should be inhibited, especially in subequatorial zones (Eastoe and Gustin, 1996), favoring eutrophication. Initiation of a short-lived regional anoxia event could be triggered by massive biomass extinction, favored by major input of C_{org} from land and an increase of $\delta^{13}C$ values as has been recorded by Kaiser et al. (2006). In fact, the observed increase in the global $\delta^{34}S$ values of seawater sulfate at the D–C boundary (Caplan and Bustin, 1999; Claypool et al., 1980) can be attributed to high rates of biogenic reduction and precipitation of pyrite during this anoxic period. Furthermore, McLaren and Goodfellow (1990) have claimed that most of these catastrophic events are related to meteoritic impacts, but no geologic nor geochemical evidence of such an event has been found in the Iberian Pyrite Belt.

Our hypothesis is that volcanism was accompanied by dramatic climatic changes at a regional scale. The onset of extensive subaerial volcanic activity was accompanied by an increase in the geothermal gradient and the formation of large clouds of volcanic ash and dark winter as well as acid rain that caused the devastation of large forests and further extensive erosion. This should produce a dramatic decrease of continental biomass, ocean eutrophication, formation of anoxic bottoms and onset of favorable conditions for massive biogenic reduction of seawater sulfate. Alternatively, rapid topographic changes related to basin configuration during oblique collision, with depression–submersion or uplift of large areas, may also have produced severe deforestation by the reconfiguration of the regional hydrology and fluvial networks. The destruction of the forests may also have resulted in an over-flux of atmospheric CO_2, which would not have been readily buffered due to widespread biomass loss in the ocean.

Preserved volcanogenic massive sulfide deposits of late Devonian–early Carboniferous age are mainly restricted to the Iberian Pyrite Belt and the D–C transition is not an epoch of relevant global volcanic activity. All these processes are likely interconnected to the global changes that led to the mass extinction of plants and animals at the D–C boundary. However, to what extent this forest devastation had global significance is outside the scope of this paper. Despite being an attractive option, we cannot be certain that the geographically restricted volcanism and hydrothermal activity had such a dramatic impact on the global climate during the D–C boundary. More likely, volcanism and hydrothermal activity are a consequence of the major geotectonic changes that took place at the D–C transition in the region of the Iberian Pyrite Belt (Fig. 7).

6. Conclusions

The geochemistry of shale hosting the giant massive sulfide deposits of the southern Iberian Pyrite Belt shows that there is a close relationship between the presence of biomarkers indicative of vascular plants, and the ore deposits. The formation of the massive sulfide deposits is believed to be the result of the microbial activity driven by the degradation of plant organic matter sourced on the adjacent continent.

The appearance of large amounts of tree detritus coincides in time with the D–C boundary and the onset of volcanism in the area, suggesting a relationship between catastrophic events, major geotectonic changes and formation of a large ore province. The formation of the giant massive sulfide deposits of the Iberian Pyrite Belt was due to the unusual combination of different crustal processes that took place at or near the Devonian–Carboniferous boundary, with superposition of likely independent, but probably intimately interconnected macro- to microscale geologic processes that occurred in a time span of less than 1 Ma. They include early continent collision, formation of shallow marine basins, volcanism and hydrothermal activity during the early part of the Variscan orogeny, dewatering of sedimentary basins, formation of anoxic bottoms, extensive biomass destruction and flourishing of extremophile biogenic activity. The availability of large amounts of biogenically derived sulfur was the ultimate key for ore formation in the Iberian Pyrite Belt. Without that process, controlled itself by the devastation of large continental forests, metals contained in the hydrothermal fluids would have been lost from the basin, preventing the formation of these giant deposits. Thus, our data strongly suggest that the massive sulfide deposits of the Iberian Pyrite Belt are directly related a major tectonic, climatic and biological crisis.

Acknowledgements

This work was supported by internal projects of the CAB and the IGME and the projects DGI-FEDER CGL2006-0378, ESP2006-556 and AYA2009-11681 of the Research and Innovation Ministry of Spain. We thank A. H. Knoll, H. Ohmoto, C. Conde, W. D. Goodfellow, C. Heinrich, F. Velasco and, especially, N.C. White their suggestions and comments. We extend our sincere thanks to the editor, M.L. Delaney, and two anonymous referees for their suggestions, comments and help during the editing process.

References

Algeo, T.J., Scheckler, S.E., Maynard, J.B., 2001. Effects of early vascular land plants on weathering processes and global chemical fluxes during the Middle and Late Devonian. In: Gensei, P.G., Edwards, D. (Eds.), Plants Invade the Land: Evolutionary and Environmental Perspectives. Columbia University Press, New York, pp. 83–102.

Please cite this article as: Menor-Salván, C., et al., Association between catastrophic paleovegetation changes during Devonian–Carboniferous boundary and the formation of giant massive sulfide deposits, Earth Planet. Sci. Lett. (2010), doi:10.1016/j.epsl.2010.09.020

Almodovar, G.R., Saez, R., Pons, J.M., Maestre, A., Toscano, M., Pascual, E., 1998. Geology and genesis of the Aznalcollar massive sulphide deposits, Iberian Pyrite Belt, Spain. Mineralium Deposita 33, 111–136.

Aparecida Vieira, S., Ferreira Alves, L., Aidar, M., Spinelli Araújo, L., Baker, T., Ferreira Bástida, J.L., Cruz Campos, M., Barbosa Casmargo, P., Chave, J., Carvalho Delitti, W.B., Higuchi, N., Honorio, E., Joly, C.A., Keller, M., Martinelli, L.A., Arcoverde de Mattos, E., Metzker, T., Phillips, O., Maes dos Santos, F.A., Takako Shimabukuro, M., Silveira, M., Trumbore, S.E., 2009. Estimation of biomass and carbon stocks: the case of the Atlantic Forest. Biota Neotrop. 8, 21–29.

Bai, Y., Wang, Y., Fang, X., Kenig, F., Miao, Y., Wang, Y., 2006. Branched alkanes with quaternary carbon atoms in Chinese soils: potential environmental significance. Chin. Sci. Bull. 51, 1115–1122.

Barrie, C.T., Amelin, Y., Pascual, E., 2002. U-Pb geochronology of VMS mineralization in the Iberian Pyrite Belt. Miner. Deposita 37, 684–703.

Bastow, T.P., Singh, R.K., van Aarssen, B.K.G., Alexander, R., Kagi, R.I., 2001. 2-methylretene in sedimentary material: a new higher plant biomarker. Org. Geochem. 32, 1211–1217.

Caplan, M.L., Bustin, R.M., 1999. Devonian–Carboniferous Hangenberg mass extinction event, widespread organic-rich mudrock and anoxia: causes and consequences. Palaeogeogr. Palaeoclimatol. Palaoecol. 148, 187–207.

Chave, J., Andalo, C., Brown, S., Cairns, M., Chambers, J., Eamus, D., Fölster, H., Fromard, F., Higuchi, N., Kira, T., Lescure, J.P., Nelson, B., Ogawa, H., Puig, H., Riera, B., Yamakura, T., 2005. Tree allometry and improved estimation of carbon stocks and balance in tropical forests. Oecologia 145, 87–99.

Claypool, G.E., Holser, W.T., Kaplan, I.R., Sakai, H., Zak, I., 1980. The age curves of sulfur and oxygen isotopes in marine sulfate and their mutual interpretation. Chem. Geol. 28, 199–260.

Dunning, G.R., Diez Montes, A., Matas, J., Martin Parra, L.M., Almarza, J., Donaire, M., 2002. Geocronología U/Pb del volcanismo ácido y granitoides de la Faja Pirítica Ibérica (Zona Surportuguesa). Geogaceta 32, 127–130.

Eastoe, C.J., Gustin, M.M., 1996. Volcanogenic massive sulfide deposits and anoxia in the Phanerozoic waters. Ore Geol. Rev. 10, 179–197.

Falcon-Lang, H.J., 2004. Early Mississipian lycopsid forest in a delta-plain setting at Norton, near Sussex, New Brunswick, Canada. J. Geol. Soc. 161, 969–981.

Fleck, S., 2002. Organic geochemistry in a sequence stratigraphic framework. The siliciclastic shelf environment of Cretaceous series, SE France. Org. Geochem. 33, 1533–1537.

Gong, Y.M., Shi, G.R., Weldon, E.A., Du, Y.S., Xu, R., 2008. Pyrite framboids interpreted as microbial colonies within the Permian zoophycos spreiten from southeastern Australia. Geol. Mag. 145, 95–103.

Gonzalez, F., 2005. Las pizarras negras del límite Devónico/carbonífero de la Faja Pirítica Ibérica (SO de España). Estudio bioestratigráfico e implicaciones sobre la paleogeografía de la cuenca y el origen de las mineralizaciones de sulfuros, PhD Thesis, 200 p. Huelva University.

Gonzalez, F., Moreno, C., Santos, A., 2006. The massive sulphide event in the Iberian Pyrite Belt: confirmatory evidence from the Sotiel–Coronada Mine. Geol. Mag. 143, 821–827.

Goodfellow, W.D., 1987. Anoxic stratified oceans as a source of sulphur in sediment hosted stratiform Zn–Pb deposits (Selwyn basin, Yukon, Canada). Chem. Geol. 65, 359–382.

Goodfellow, W.D., Jonasson, I.R., 1984. Ocean stagnation and ventilation defined by $\delta^{34}S$ secular trends in pyrite and barite, Selwyn Basin, Yukon. Geology 12, 583–586.

Herzig, P.M., Hannington, M.D., 1995. Polymetallic massive sulfides at the modern seafloor. A review. Ore Geol. Rev. 10, 95–115.

Jackson, F.D., Jin, X., Schmitt, J.G., 2009. Fungi in a lower Cretaceous turtle egg from China: evidence of ecological interactions. Palaios 24, 840–845.

Johnson, K.R., Nichols, D., Labandeira, C., Pearson, D., 2000. Devastation of terrestrial ecosystems at the K–T boundary in North America: the first calibrated record of plant and animal response to the Chicxulub impact. Catastrophic Events and Mass Extinctions: Impacts and Beyond, Vienna, pp. 85–86, LPI Contribution No. 1053, Lunar and Planetary Institute, Houston.

Kaiser, S.I., Steuber, T., Becker, T., Joachimski, M.M., 2006. Geochemical evidence for major environmental change at the Devonian–Carboniferous boundary in the Carnic Alps and the Rhenish Massif. Palaeogeogr. Palaeoclimatol. Palaeoecol. 240, 146–160.

Kenig, F., 2003. Branched aliphatic alkanes with quaternary substituted carbon atoms in modern and ancient geologic samples. Proc. Nat. Acad. Sci. USA 1000, 12554–12558.

Kenig, F., 2005. Structure and distribution of branched aliphatic alkanes with quaternary carbon atoms in Cenomanian and Turonian black shales of Pasquia Hills (Saskatchewan, Canada). Org. Geochem. 36, 117–138.

Labes, A., Schönheit, P., 2001. Sugar utilization in the hyperthermophilic, sulfate-reducing archaeon *Archaeoglobus fulgidus* strain 7324: starch degradation to acetate and CO_2 via a modified Embden–Meyerhof pathway and acetyl-CoA synthetase (ADP-forming). Arch. Microbiol. 176, 329–338.

Leistel, J.M., Marcoux, E., Thieblemont, D., Quesada, C., Sanchez, A., Almodovar, G.R., Pascual, E., Saez, R., 1998. The volcanic-hosted massive sulphide deposits of the Iberian Pyrite Belt. Review and preface to the special issue. Miner. Deposita 33, 2–30.

Lydon, J.W., 1988. Volcanogenic massive sulphide deposits: II. genetic models. In: Roberts, R.G., Sheanan, P.A. (Eds.), Ore deposit models, Geoscience Canada: reprint series, 3, pp. 43–65.

Marcoux, E., Moelo, Y., Leistel, J.M., 1980. Bismuth and cobalt minerals: indicators of stringer zones to massive-sulfide deposits, South Iberian Pyrite Belt. Miner. Deposita 31, 1–26.

McLaren, D.J., Goodfellow, W.D., 1990. Geological and biological consequences of giant impacts. Ann. Rev. Earth Planet. Sci. 18, 123–171.

Monetti, M.A., Scranton, M.I., 1992. Fatty acid oxidation in anoxic marine sediments: the importance of hydrogen sensitive reactions. Biogeochemistry 17, 23–47.

Moreno, C., Sierra, S., Saez, R., 1996. Evidence for catastrophism at the Famennian–Dinantian boundary in the Iberian Pyrite Belt. In: Strogen, P., Somervilee, I.D., Jones, G.L. (Eds.), Recent Advances in Lower Carboniferous Geology: Geological Society London, pp. 153–162.

Nägler, T., 1990, Sm-Nd, Rb-Sr and common lead isotope geochemistry on fine-grained sediments of the Iberian Massif: Unpub. Doctoral thesis, Swiss Federal Institute Technology, 139 p.

Ohmoto, H., 1996. Formation of volcanogenic massive sulfide deposits: the Kuroko perspective. Ore Geol. Rev. 10, 135–177.

Oliveira, J.T., Pereira, Z., Carvalho, P., Pacheco, N., Korn, D., 2003. Stratigraphy of the tectonically imbricated lithological succession of the Neves Corvo Mine Region. Iberian Pyrite Belt. Implications for regional basin dynamics. Miner. Deposita 39, 422–436.

Otto, A., Simoneit, B.R.T., 2001. Chemosystematics and diagenesis of terpenoids in fossil conifer species and sediment from the Eocene Zeitz formation, Saxony, Germany. Geochim. Cosmochim. Acta 65, 3505–3527.

Pereira, Z., Saez, R., Pons, J.M., Oliveira, J.T., Moreno, C., 1996. Edad devónica (Struniense) de las mineralizaciones de Aznalcóllar (Faja Pirítica Ibérica) en base a palinología. Geogaceta 20, 1609–1612.

Peters, K.E., Walters, C.C., Moldowan, J.M., 2005. The Biomarker Guide, second edition. Volume 2: biomarkers and isotopes in petroleum exploration and Earth history. Cambridge University Press, Cambridge.

Relvas, J.M.R.S., Tassinari, C.C.G., Munha, J., Barriga, F.J.A.S., 2001. Multiple sources for ore forming fluids in the Neves Corvo VHMS deposit of the Iberian Pyrite Belt (Portugal): Strontium, Neodymium and Lead isotope evidence. Mineralium Deposita 36, 416–427.

Sato, T., 1972. Behaviours of ore forming solutions in seawater. Min. Geol. 22, 31–42.

Sepkoski, J.J., 1996. Patterns of Phanerozoic extinction: a perspective from global data bases. In: Walliser, O.H. (Ed.), Global Events and Event Stratigraphy in the Phanerozoic. Springer, Berlin, pp. 35–51.

Silva, J.B., Oliveira, J.T., Ribeiro, A., 1990. Structural outline of the South Portuguese Zone. In: Dallmeyer, R.D., Martinez García, E. (Eds.), PreMesozoic Geology of Iberia. Springer, Heidelberg, pp. 348–362.

Solomon, M., Tornos, F., Large, R.R., Badham, J.N.P., Both, R.A., Zaw, K., 2004. Zn–Pb–Cu volcanic-hosted massive sulphide deposits: criteria for distinguishing brine pool-type from black smoker-type sulphide deposition. Ore Geol. Rev. 25, 259–284.

Stetter, K.O., 1999. Extremophiles and their adaptation to hot environments. FERS Lett. 452, 22–25.

Streel, M., Brice, D., Mistiaen, B., 2006. Strunian. Geol. Belg. 9, 105–109.

Tornos, F., 2006. Environment of formation and styles of volcanogenic massive sulfides: the Iberian Pyrite Belt. Ore Geol. Rev. 28, 259–307.

Tornos, F., Gonzalez Clavijo, E., Spiro, B.F., 1998. The Filón Norte orebody (Tharsis, Iberian Pyrite Belt): a proximal low-temperature shale-hosted massive sulphide in a thin-skinned tectonic belt. Miner. Deposita 33, 150–169.

Tornos, F., Heinrich, C.A., 2008. Shale basins, sulfur-deficient ore brines, and the formation of exhalative base metal deposits. Chem. Geol. 247, 195–207.

Tornos, F., Solomon, M., Conde, C., Spiro, B.F., 2008. Formation of the Tharsis massive sulfide deposit, Iberian Pyrite Belt: geological, lithogeochemical, and stable isotope evidence for deposition in a brine pool. Econ. Geol. 103, 185–214.

Van Aarssen, B.G.K., Alexander, R., Kagi, R.I., 1996. The origin of Barrow Sub-basin crude oils: a geochemical correlation using land plant biomarkers. APPEA J. 36, 465–476.

Van Aarssen, B.G.K., Alexander, R., Kagi, R.I., 2000. Higher plant biomarkers reflect paleovegetation changes during Jurassic times. Geochim. Cosmochim. Acta 64, 1417–1424.

Velasco, F., Sanchez España, J., Boyce, A., Fallick, A.E., Saez, R., Almodovar, G.R., 1998. A new sulphur isotopic study of some Iberian Pyrite Belt deposits: evidence of a textural control on some sulphur isotope compositions. Miner. Deposita 34, 1–18.

Wilf, P., Johnson, K.R., 2004. Land plant extinction at the end of the Cretaceous: a quantitative analysis of the North Dakota megafloral record. Paleobiology 30, 347–368.

Please cite this article as: Menor-Salván, C., et al., Association between catastrophic paleovegetation changes during Devonian–Carboniferous boundary and the formation of giant massive sulfide deposits, Earth Planet. Sci. Lett. (2010), doi:10.1016/j.epsl.2010.09.020